PROPERTIES OF MAPS RELATED TO FLOWS AROUND A SADDLE POINT

P. SZÉPFALUSY[1] and T. TÉL[2]†

[1]*Central Research Institute for Physics, P.O. Box 49 H-1525 Budapest 114, Hungary, and Institute for Theoretical Physics, Eötvös University, Budapest, Hungary*
[2]*Fachbereich Physik, Universität Essen GHS D-4300 Essen 1, Fed. Rep. Germany*

General properties of maps associated with systems in which trajectories of the flow get close to a hyperbolic fixed point with a two-dimensional stable and a one-dimensional unstable manifold are examined in the chaotic region.

Exponents characterizing power law singular behaviour of the Jacobian, of the shape of and of the stationary probability distribution on the chaotic attractor are expressed in terms of the ratios of the eigenvalues of the linearized flow at the hyperbolic point. Emphasis is laid on the study of the limiting case of strong dissipation leading to a simple one-dimensional attractor but to a dynamics with interesting features.

1. Introduction and summary

The relation between the flow of a continuous dynamical system in phase space and the discrete map generated by it on a Poincaré surface plays an essential role in the theory of dynamical systems. It is a basic problem, however, that the recursion relations of the map cannot, in general, be deduced without solving the equations of motion. By this reason, approximate maps have often been applied by assuming that the Jacobian of the map can be taken as constant [1, 2]. In the present paper we show that this is not allowed in those cases when typical trajectories go close to a hyperbolic point, and investigate several properties of this type of maps in the region of parameter values where they exhibit chaotic iterations.

A well-known example of such continuous systems is the Lorenz model near the standard values of the parameters ($\sigma = 10$, $b = \frac{8}{3}$, $r = 28$) [3]. The relation between the flow and the map has been extensively studied both near $r = 28$ [4–9] and at

† On leave from the Institute for Theoretical Physics, Eötvös University, Budapest, Hungary.

much higher values of the control parameter [10]. A special property of the strange attractor near $r = 28$ is the Cantor book structure [5, 6, 11] which means that the sheets of the attractor are bound together along the unstable invariant curve of the origin. Therefore, on an associated Poincaré map the branches of the two-dimensional strange attractor are pinched at each point where the unstable manifold of the origin intersects the surface [6–8, 12]. The Cantor book structure is a consequence of the fact that the flow on the strange attractor approaches the origin which has a two-dimensional invariant stable manifold and, therefore, trajectories depart in the direction of the unstable invariant curve. This is a topological effect. There is a dynamical consequence, too, as the motion slows down in the vicinity of the origin, thus, the hyperbolicity is not uniform, the attractor cannot be an axiom A one [13]. A third manifestation of the same fact is that the quasi one-dimensional map defined by the recursion of the amplitude maxima of one of the variables (e.g. $Z(t)$) has a singular form [3]. The exponent of the leading power appearing in it is related to two eigenvalues of the linearized motion around the

origin [14]. The mechanism of the onset of chaos has also peculiar properties owing to the singular nature of the flow [11, 14–18]. It has to be emphasized that the feature that typical trajectories pass near a hyperbolic point can be characteristic for a whole class of dynamical systems [12, 15–18] and thus, the investigations, not restricted to the Lorenz model, might have a broad relevance.

In this paper we concentrate on the properties of the chaotic motion exhibited by such systems. Our main results can be summarized as follows. We show that the Jacobian of the map has a power law singularity when approaching the intersection line of the Poincaré surface with the stable manifold of the hyperbolic point. The critical exponent characterizing this singularity is obtained as the divergence of the flow at the hyperbolic point divided by the positive eigenvalue. Furthermore, all the branches of the strange attractor on the Poincaré plane are shown to approach a straight line at the backbone of the Cantor book according to a common power law behaviour the exponent of which is given by the ratio of the two negative eigenvalues. Consequently, the strange attractor ends with a sharp peak at the backbone point (whether it happens from one or from two sides depends also on the ratio of the two negative eigenvalues). Besides the local shape near the backbone point an approximate global form is obtained by means of a perturbative method starting from the one-dimensional case. Another consequence of the singular feature shows up in the stationary probability distribution at the backbone of the Cantor book. The density exhibits, along each of the branches, a power law behaviour specified now by the ratio of the larger negative eigenvalue and the positive one. The first correction term after the leading one is also evaluated to the density.

We have carried out detailed examinations at the parameter setting when the Jacobian of the map vanishes identically, which corresponds to the limit of strong dissipation. Then, the motion, after the first step, takes place on two straight lines with a coupled dynamics on them. The master equation

for the stationary probability distribution is derived, and applied to obtain the singular part of the invariant density. When the system possesses the same symmetry property as the Lorenz model the master equation becomes equivalent with that of a suitable constructed continuous 1D map which is, in general, nonsymmetric. Our most remarkable findings are connected to the case when the value of the ratio of the two negative eigenvalues is opposite to that of the Lorenz model exhibiting chaotic motion. Namely, then the 1D map has a quadratic maximum and at the backbone point a positive Schwarzian derivative or a vanishing slope. According to our numerical simulations a unique invariant probability distribution may exist for these maps in the situation when the maximum point is mapped in two steps to an unstable fixed point.

The paper is organized as follows. In section 2 we derive the local form of the Poincaré map and determine the exponent of its Jacobian. Then, we investigate the dynamics in the limit of strong dissipation. Section 4 is devoted to the study of the shape of the strange attractor. The last section deals with the evaluation of the probability density along the fibres of the strange attractor at the backbone of the Cantor book. Appendix A contains an example where the stationary density can be calculated exactly in the limit of strong dissipation. In appendix B we present a general class of maps in which singular Jacobian, Cantor book structure and singular probability density may appear simultaneously.

2. Two-dimensional return map

We consider a three-dimensional dynamical system with variables X_i, $i = 1, 2, 3$ the time evolution of which is governed by autonomous ordinary differential equations. Let the origin of the phase space X_1, X_2, X_3 be a hyperbolic point with a two-dimensional stable manifold and a one-dimensional unstable manifold, $W^u(0)$. For the sake of simplicity, the variables X_i are chosen to

be the normal modes of the linearized equations around the origin with eigenvalues λ_i, so that X_1 belongs to the unstable mode, i.e. $\lambda_1 > 0$ but λ_2, $\lambda_3 < 0$. Consequently, a small volume of the phase space around the origin changes in time as $\exp(\Lambda t)$, where

$$\Lambda = \sum_{i=1}^{3} \lambda_i \qquad (2.1)$$

denotes the divergence of the flow at $X_i = 0$. Note, that the coordinate system X_1, X_2, X_3 is, in general, not rectangular.

The Poincaré surface is chosen as the $X_3 = z = $ const plane where z is adjusted in such a way that the unstable manifold of the hyperbolic point should intersect the plane several times. In a certain reference frame on this plane the coordinates are denoted by x, y. We use the convention that only intersections from above belong to the map. The points D^+ and D^- will be of special importance, where D^+ (D^-) represents the first intersection point between the $X_3 = z$ plane and that branch of the unstable manifold $W^u(0)$ which emanates into the positive (negative) X_1 direction (fig. 1).

The standard procedure of obtaining the singular features of the map consists of a linearization of the flow in the vicinity of the saddle point and of postulating a return mechanism in course of which typical trajectories do not pass close to any other singular point [19, 5, 7, 14, 8, 16]. As the plane $X_3 = z$ is generally outside of the region where the motion can be well approximated by the linearized equations around the hyperbolic fixed point, we introduce an auxilary surface defined by $X_3 = Z$, where Z is a sufficiently small constant. The reference frame X, Y on this surface is chosen in such a way that the origin $X = Y = 0$ is the intersection point of the plane and the X_3 axis, and the X (Y) axis is parallel with the X_1 (X_2) axis.

The trajectory passing through $P = (x, y)$ crosses the $X_3 = Z$ plane at a certain point (X, Y). More generally, the flow generates a map $X = X(x, y)$, $Y = Y(x, y)$ between the two surfaces,
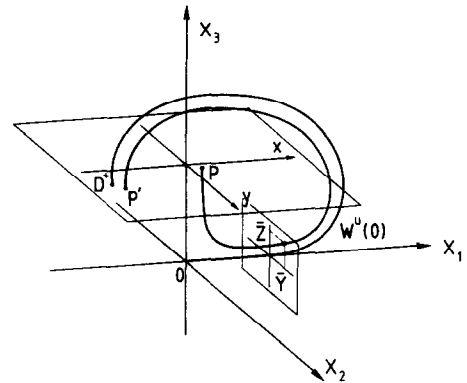

Fig. 1. The branch of the unstable manifold $W^u(0)$ which emanates in the positive X_1 direction, and a trajectory passing near the hyperbolic point at the origin.

where $X(x, y)$ and $Y(x, y)$ are smooth functions of their variables since no singular point lies between the planes $X_3 = z$ and $X_3 = Z$. The actual form of these functions may depend on z and Z as parameters. It is to be noted that the line $X = 0$ of the $X_3 = Z$ plane is by construction the intersection line with the stable manifold of the hyperbolic point. Consequently, the curve on the $X_3 = z$ plane defined by $X(x, y) = 0$ represents the intersection curve between the Poincaré surface and the stable manifold of the hyperbolic point. It is natural to define the origin $x = y = 0$ on the Poincaré plane as the preimage of the origin of the auxilary plane, i.e. by the requirement $X(x, y) = Y(x, y) = 0$.

Trajectories passing close to the hyperbolic point must start from the neighbourhood of the stable manifold. As, however, the Y-axis points in a contracting direction, and the strange attractor must be of finite size, an appropriate choice for Z always guarantees that both coordinates X, Y of the intersection with the auxilary plane will be small. The subsequent motion of the point $(X, (x, y), Y(x, y), Z)$ is thus described by the solution of the linearized equations, i.e. by

$$X_1(t) = X(x, y)\exp(\lambda_1 t),$$
$$X_2(t) = Y(x, y)\exp(\lambda_2 t), \qquad (2.2)$$
$$X_3(t) = Z\exp(\lambda_3 t).$$

Consequently, a plane $X_1 = \overline{X}$, where $\overline{X}$ still belongs to the linear region and has the same sign as $X(x, y)$, is reached at $X_2 = \overline{Y}(x, y)$, $X_3 = \overline{Z}(x, y)$ where

$$\overline{Y}(x, y) = Y(x, y)|X(x, y)/\overline{X}|^{|\lambda_2|/\lambda_1}$$
$$\overline{Z}(x, y) = Z|X(x, y)/\overline{X}|^{|\lambda_3|/\lambda_1}. \qquad (2.3)$$

(See fig. 1; note, however, that for the sake of clarity the auxilary plane is not shown there.)

As, after having left the surface $X_1 = \overline{X}$, the trajectory does not pass near any singular point, the deviation between the next intersection $P' = (x', y')$ with the Poincaré surface and D^+ (D^-), if $X(x, y) > 0$ (if $X(x, y) < 0$), is an analytic function of $\overline{Y}$ and $\overline{Z}$. For small values of X and Y it is sufficient to keep the first terms of the Taylor expansion only, apart from exceptional cases when their coefficients vanish. Thus, we find as a typical form of the map near $X(x, y) = 0$

$$x' = \left(u + a_{11}|X(x, y)|^\beta \right) \operatorname{sgn}\left(X(x, y) \right)$$
$$\qquad + a_{12}Y(x, y)|X(x, y)|^\delta$$
$$y' = \left(v + a_{21}|X(x, y)|^\beta \right) \operatorname{sgn}\left(X(x, y) \right) \qquad (2.4)$$
$$\qquad + a_{22}Y(x, y)|X(x, y)|^\delta,$$

where

$$\beta = |\lambda_3|/\lambda_1, \quad \delta = |\lambda_2|/\lambda_1, \qquad (2.5)$$

$\operatorname{sgn}(X)$ denotes the sign of X, the coefficients a_{ij} are constants, and u, v are the coordinates of the point D^+. For the sake of simplicity we assumed by writing down (2.4) that the equations of motion are invariant under the transformation $X_1 \to -X_1$, $X_2 \to -X_2$, $X_3 \to X_3$ which is a well-known property of the Lorenz model. This assumption simplifies the presentation in the following but does not influence our main results except at the end of section 3 where the symmetry property is essential for the consideration as emphasized there.

The Jacobian of the map on the Poincaré surface, which is the area contracting ratio in non-rectan-gular coordinate systems as well, is obtained as

$$J(x, y) = (a_{11}a_{22} - a_{12}a_{21})A(x, y)\beta|X(x, y)|^\eta, \qquad (2.6)$$

with

$$\eta = -\Lambda/\lambda_1 = \beta + \delta - 1, \qquad (2.7)$$

where (2.1) and (2.5) have been used. $A(x, y)$ denotes here the Jacobian of the map generated by the flow between the planes $X_3 = z$ and $X_3 = Z$:

$$A(x, y) = X_x(x, y)Y_y(x, y) - X_y(x, y)Y_x(x, y), \qquad (2.8)$$

where $X_x(x, y)$ stands for the partial derivative of the function X with respect to x, etc. $A(x, y)$ depends smoothly on the variables as it belongs to a nonsingular map. This is, however, not the case with $J(x, y)$ itself. As we have seen, $X(x, y)$ vanishes along the intersection line between the stable manifold of the hyperbolic point and the Poincaré surface, which makes $J(x, y)$ to be non-analytic. It follows from (2.7) that the nature of the nonanalytic behaviour is strongly related to the divergence of the flow near the origin. $J(x, y)$ vanishes as $X(x, y)$ tends to zero if the flow is locally dissipative ($\Lambda < 0$) and diverges if the flow is locally expanding ($\Lambda > 0$) at the hyperbolic point.

If one applies the general results for the example of the Lorenz model near $r = 28$, and uses the well-known expressions of the eigenvalues (see e.g. [14]), one obtains

$$\eta = \frac{2(b + \sigma + 1)}{\left[(1 + \sigma)^2 + 4\sigma(r - 1) \right]^{1/2} - (1 + \sigma)}. \qquad (2.9)$$

At the standard parameter values quoted above $\eta = 1.1555$ while the other two exponents given by (2.5) turn out to be $\beta = 0.2255$, $\delta = 1.9300$. It can be easily seen that the chaotic attractor appearing in the Lorenzian equation introduced by Rössler [12] is found at parameter values which yield, according to (2.7), $\eta < 0$.

The form of the map (2.4) simplifies considerably if we consider the recursions only in a small region around the origin of the Poincaré surface. The functions $X(x, y)$ and $Y(x, y)$ are then given as linear combinations of x and y, and we may choose the reference frame such that $X(x, y)$ is proportional to x and $Y(x, y)$ to y in the new variables. After having appropriately rescaled the length scales, one arrives at

$$x' = \left(-1 + a|x|^{\beta}\right)\operatorname{sgn}(x) + cy|x|^{\delta},$$
$$y' = \left(d + |x|^{\beta}\right)\operatorname{sgn}(x) + by|x|^{\delta}, \tag{2.10}$$

with an x-dependent Jacobian

$$J(x) = (ab - c)\beta|x|^{\eta}, \tag{2.11}$$

where the exponents have been given by (2.5) and (2.7). The appearance of -1 in (2.10) indicates that the point D^+ is supposed to lie below the v-axis of the Poincaré surface (fig. 1). Note that the constants a, b, c, d are "nonuniversal" parameters: they are connected with the nonlinear part of the equations of motion and may depend on the choice (the z coordinate) of the Poincaré cross-section, too. In the following the parameter region $a > 0$, $b \geq 0$, $ab \geq c$ will be investigated.

The general form of the Poincaré map contains, of course, additional terms, analytic or less singular as those given already by eq. (2.10). In order to illustrate the consequences of the singular feature of the map, however, it is sufficient to keep the most singular part. Therefore, we consider in the following the map obtained by extending the validity of eq. (2.10) to the whole plane. More precisely, we regard the map (2.10) as a model which is designed to simulate some essential features of a flow around a saddle point. In particular, we will be interested in metric properties.

The strange attractor found in numerical simulations of (2.10) possesses Cantor book structure (fig. 2). This remains valid even if the Jacobian diverges at $x = 0$ ($\eta < 0$). By varying the exponents β and δ the shape of the strange attractor may change drastically. This goes back to a change
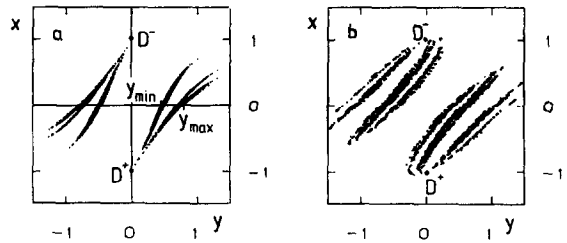

Fig. 2. The strange attractor of the map (2.10) obtained in a numerical simulation after 2000 steps. a) $\beta = 0.3$, $\delta = 0.5$, $a = 1.7$, $b = 0.5$, $c = d = 0$; b) $\beta = 0.6$, $\delta = 0.2$, $a = 1.5$, $b = 0.7$, $c = 0.25$, $d = 0$.

of the local form at the backbone of the Cantor book, i.e. at $D^{\pm}$. Numerical experience suggests that also some metric properties of the map depend strongly on the exponents β, δ. Fig. 2 illustrates that for sufficiently small values of β or δ the density of dots is extremely low at the backbone of the Cantor book, i.e. the invariant probability density seems to vanish at $D^{\pm}$. A quantitative description of these observations will be given later in this paper.

3. The limit of extremely strong dissipations

Before studying the general properties of the two-dimensional map (2.10), it is worth starting with a discussion of the special case characterized by an identically vanishing Jacobian and, for this reason, by an attractor of fractal dimensionality not larger than 1. This is always the case approximately if the underlying flow is strongly dissipative in the whole phase space.

Thus, we choose in this section the parameters in such a way that $c = ab$ is fulfilled. It follows then from (2.10) that any starting point jumps immediately on one of the straight lines $x = ay \mp (1 + ad)$. The attractor is confined then by a segment with $-\Delta \leq y - d \leq e$ on the lower branch and by another one with $-e \leq y + d \leq \Delta$ on the upper branch. The values of Δ and e follow from the dynamics along the two lines.

Using the aforementioned relation between x and y as well as (2.10) we may express x' in terms

of x. For $x > 0$ we find

$$x' + 1 = af_{\pm}(x) \equiv ax^{\beta} + b(x \pm (1 + ad))x^{\delta}. \tag{3.1}$$

The y' coordinate is then determined by x' through

$$y' = d + (x' + 1)/a. \tag{3.2}$$

The equations for $x < 0$ can be obtained by turning the signs of all variables into negative. According to the original description $+$ $(-)$ is to be taken in (3.1) if the point (x, y) is on the lower (upper) branch. Once, however, a point is situated on the lower (upper) branch, the x-coordinate of its preimage had to be positive (negative). Thus, the sign in (3.1) is identical with that of the preimage of x.

According to the definition of Δ and e as parameters characterizing the endpoints of the segment containing the attractor, the domain of $f_{\pm}$ is given by

$$f_{+}: \quad 0 \leq x \leq ae - 1, \tag{3.3}$$

$$f_{-}: \quad 0 \leq x \leq 1 + a\Delta. \tag{3.4}$$

The quantity $-1 - a\Delta$ should be the minimum of x' for positive values of x. Therefore, if $f_{-}(x)$ possesses a negative minimum (e.g. for $\delta < \beta$) $\Delta = -(f_{-})_{\min}$, otherwise $\Delta = 0$. The point $x = 1 + a\Delta$ turns out to be mapped on the endpoint of the f_{-} branch, thus

$$e = (1 + a\Delta)^{\beta} + b(\Delta - d)(1 + a\Delta)^{\delta}. \tag{3.5}$$

Let us consider a general dynamics of the type of (3.1) which is specified by the following functions: $x' = \phi_{1}(x)$ for $0 < x \leq 1$, $x' = \phi_{3}(x)$ for $-1 \leq x < 0$ if the preimage of x is positive, while $x' = \phi_{2}(x)$ for $0 < x \leq 1$ and $x' = \phi_{4}(x)$ for $-1 \leq x < 0$ if the preimage is negative (see fig. 3a). We assume that the map produces chaotic iterations for almost all initial values and turn to the investigation of the stationary probability distribution. It is natural to divide the stationary density $P(x)$
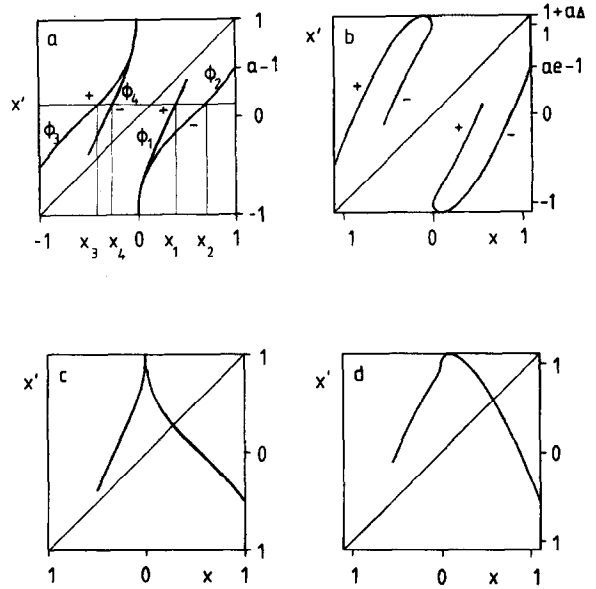

Fig. 3. The map $x_{n+1} = (-1 + a|x_{n}|^{\beta}) \text{sgn}(x_{n}) + b(x_{n} + \text{sgn}(x_{n-1}))|x_{n}|^{\delta}$ at a) $\beta = 0.5$, $\delta = 1.5$, $a = 1.5$, $b = 0.6$; b) $\beta = 1.5$, $\delta = 0.5$, $a = 1.3$, $b = 0.5$. The signs along the branches denote the sign of the preimage of x. Pictures c) and d) show the reduced map (3.18) corresponding to the parameters of pictures a) and b), respectively.

into two parts

$$P(x) = P_{+}(x) + P_{-}(x), \tag{3.6}$$

where $P_{+(-)}(x)|dx|$ is the measure of those points in $|dx|$ the preimage of which is positive (negative). As a given point x' may have two positive preimages: x_{1}, x_{2} and two negative ones x_{3}, x_{4} (figs. 3a, b) the master equation for the stationary distribution contains now two coupled equations. For $|x'| \leq 1$ they read

$$P_{+}(x')|dx'| = P_{+}(x_{1})|dx_{1}| + P_{-}(x_{2})|dx_{2}|,$$
$$P_{-}(x')|dx'| = P_{+}(x_{3})|dx_{3}| + P_{-}(x_{4})|dx_{4}|, \tag{3.7}$$

or, equivalently,

$$P_{+}(x') = \frac{P_{+}(x_{1})}{|\phi_{1}'(x_{1})|} + \frac{P_{-}(x_{2})}{|\phi_{2}'(x_{2})|},$$

$$P_{-}(x') = \frac{P_{+}(x_{3})}{|\phi_{3}'(x_{3})|} + \frac{P_{-}(x_{4})}{|\phi_{4}'(x_{4})|}, \tag{3.8}$$

where ϕ_i' denotes the derivative of ϕ_i. In a situation corresponding to fig. 3b one finds a region for $x' > 1$ where both preimages of x' belong to the branch $x' = \phi_3(x)$. In this region, therefore,

$$P_-(x') = \frac{P_+(x_3)}{|\phi_3'(x_3)|} + \frac{P_+(x_4)}{|\phi_3'(x_4)|} \qquad (3.9)$$

is valid. Similarly, for $x' < -1$

$$P_+(x') = \frac{P_-(x_1)}{|\phi_2'(x_1)|} + \frac{P_-(x_2)}{|\phi_2'(x_2)|}. \qquad (3.10)$$

Appendix A contains a simple example where the stationary density and the Lyapunov number can be exactly calculated.

The terms appearing on the right hand side of $P_+(x')$ or $P_-(x')$ can be interpreted as contributions from different branches or from different parts of the same branch. Thus, for example,

$$P_+^{(1)}(x') = \frac{P_+\left(\phi_1^{-1}(x')\right)}{\left|\phi_1'\left(\phi_1^{-1}(x')\right)\right|}, \qquad (3.11)$$

where ϕ_1^{-1} denotes the inverse of ϕ_1, represents the contribution of the upper branch to $P_+(x')$ (from the neighbourhood of x_1).

In the particular case of (2.10) with $c = ab$ the functions $\phi_i(x)$ are given by

$$
\begin{aligned}
\phi_1(x) &= -1 + af_+(x), \\
\phi_2(x) &= -1 + af_-(x), \quad x > 0, \\
\phi_3(x) &= 1 - af_-(-x), \\
\phi_4(x) &= 1 - af_+(-x), \quad x < 0,
\end{aligned}
\qquad (3.12)
$$

where $f_\pm(x)$ is defined in (3.1). We assume that the densities extend over the whole segments (3.3), (3.4) which is the case according to our numerical simulations at parameter values like those of fig. 3. Our aim is now to calculate the asymptotic form of the stationary distribution for $x' \to \pm 1$, which

corresponds to the description of the probability density around the points D$^\pm$ on the x, y plane. It follows from the symmetry properties of (2.10) that

$$P_+(-x) = P_-(x), \quad P_-(-x) = P_+(x), \qquad (3.13)$$

consequently, $P(x) = P(-x)$. Therefore, it is sufficient to consider the limit $x' \to -1$. This always implies $x_1 \to 0^+$, and $P_+(x_1)$ can be replaced by $P(0)/2$ in (3.11). When solving the equation $x' = \phi_1(x_1)$ for $x' \to -1$ one finds qualitatively different forms depending on the ratio of the exponents β and δ. Accordingly, the leading behaviour of $P_+^{(1)}(x')$ depends also strongly on this ratio.

For $\beta < \delta$ x_1 is given for $x' \to -1$ by

$$
x_1 = \left(\frac{1 + x'}{a}\right)^{1/\beta}
$$
$$
\times \left[1 - \frac{1}{\beta}\frac{b}{a}(1 + ad)\left(\frac{1 + x'}{a}\right)^{(\delta - \beta)/\beta}\right]. \qquad (3.14)
$$

Therefore, (3.11) yields

$$
P_+^{(1)}(x') = \frac{P(0)}{2a\beta}\left(\frac{1 + x'}{a}\right)^{(1 - \beta)/\beta}
$$
$$
\times \left[1 - \frac{1 - \beta + \delta}{\beta}\frac{b}{a}(1 + ad)\left(\frac{1 + x'}{a}\right)^{(\delta - \beta)/\beta}\right]. \qquad (3.15)
$$

This contribution is vanishingly small for $\beta < 1$ and divergent for $\beta > 1$. The contribution of the branch $x' = \phi_2(x)$ to $P_+(x')$ is of the same form as (3.15) but b is replaced by $(-b)$.

For $\beta = \delta$ the contribution of the upper branch is equal to

$$
P_+^{(1)}(x') = \frac{P(0)}{2\beta(a + b(1 + ad))}
$$
$$
\times \left(\frac{1 + x'}{a + b(1 + ad)}\right)^{(1 - \beta)/\beta} \qquad (3.16)
$$

In the case of $\beta > \delta$ (see fig. 3b), as long as $x' > -1$, one obtains from (3.11)

$$P_+^{(1)}(x') = \frac{P(0)}{2b\delta(1 + ad)} \left(\frac{1 + x'}{b(1 + ad)} \right)^{(1-\delta)/\delta}$$

$$\times \left[1 - \frac{1 + \beta - \delta}{\delta} \frac{a}{b(1 + ad)} \right.$$

$$\left. \times \left(\frac{1 + x'}{b(1 + ad)} \right)^{(\beta-\delta)/\delta} \right], \qquad (3.17)$$

which again vanishes or diverges depending on the sign of $1 - \delta$. For $x' < -1$ only the second branch plays a role. The singular contribution to the probability distribution is then given by the right hand side of (3.17) with b replaced by $(-b)$.

The leading term in (3.15) is in accordance with the results obtained for a map $z' = 1 - a|z|^\beta$ ([20], see also [21]) and those of the Lorenz model (for $\beta < 1$) on its branched manifold [22, 23].

Two remarks are in order. First, it follows from (3.17) that the limit $b \to 0$ ($c \to 0$) cannot be taken there. A direct calculation then gives $P_+^{(1)}(x') = P(0)((1 + x')/a)^{(1-\beta)/\beta}/2a\beta$. Second, the fact that $P(x_1)$ approaches, in general, $P(0)$ linearly may influence the type of the next to leading terms. Relations (3.15), (3.17) are, therefore, valid for $|\delta - \beta| < 1$ only. For $|\delta - \beta| > 1$ the powers of the terms appearing in the square brackets of (3.15) and (3.17) are $1/\beta$ and $1/\delta$, respectively.

Alternatively, we can also give the invariant probability density $\rho(x, y)$ on the two branches of the attractor on the x, y plane. Clearly, owing to the difference in the volume element, $\rho(x, y) = P_\sigma(x)[1 + a^2]^{-1/2}$, where $\sigma = +, -$ corresponds to the lower and the upper branch, respectively.

By increasing the parameter a in (3.1), one typically reaches a value a_c where $f_+(ae - 1) = e$. Beyond this value the branch of f_+ crosses the diagonal and the motion is no more bounded. The critical case at a_c represents a boundary crises [24]: an unstable fixed point collides with the basin of the chaotic attractor. Simultaneously, the situation at a_c can be considered as a state with fully developed chaos [20] in (3.1).

Before proceeding, it is worth discussing at this point to which extent the assumed symmetry property of the system has influenced our results. It is obvious, that the basic feature of the dynamics, namely that it has a special two-step nature, remain valid in the general case and so do eqs. (3.8)–(3.10). Concerning the asymptotic behaviour given by (3.15)–(3.17), the lack of symmetry influences the prefactors but the exponents remain unchanged.

The last part of this section, however, relies heavily on the symmetry property, making a reformulation of the master equation possible. For this purpose, let us now introduce an associated 1D map by the following convention:

$$x' = H(x),$$

$$H(x) = \begin{cases} \phi_4(x), & x < 0, \\ \phi_3(-x), & x > 0, \end{cases} \qquad (3.18)$$

(see fig. 3c, d). It can be easily seen that owing to the symmetry property (3.13), the probability density $P_-(x)$ is invariant under the iteration (3.18) according to (3.8)–(3.10). The procedure is similar in spirit to Lanford's treatment of the Lorenz model [6] by regarding as identical the points symmetric with respect to the symmetry transformation of the model. This representation is well suited for discussing the basic questions of the existence of a unique stationary probability distribution with a density since this problem has extensively been studied in the case of such continuous 1D maps.

Four cases should be distinguished: a) $\beta < \delta$, $\beta < 1$ (like in the standard Lorenz model); b) $\beta < \delta$, $\beta > 1$; c) $\beta > \delta$, $\delta < 1$; d) $\beta > \delta$, $\delta > 1$. In case a) the map has a cusp, while in cases b), c) and d) it has a smooth maximum. In the former case, if the map is everywhere expanding, well-known theorems apply and the existence of the unique probability density is ensured (see [25] and references therein). In the latter cases the map can produce chaotic iterations for typical initial conditions only at particular control parameter values. The situation when the maximum point is mapped

in two steps to an unstable fixed point, i.e., when fully developed chaos can exist, has been most extensively studied. Two basic conditions under which the existence of a unique absolutely continuous invariant measure has been proven in this situation are that the first derivative of the map is nonzero except at the maximum point and that its Schwarzian derivative is negative [25, 26]. Both can be valid in case b), but in cases c) and d) the second and the first condition is violated near $x = 0$, respectively. According to our numerical simiiations, the map possesses in the fully developed chaos situation a unique probability distribution which extends over the whole interval mapped onto itself, in all four cases, despite the facts mentioned above and that in case a) the map considered was not everywhere expanding. The problem certainly requires further investigations.

4. The shape of the strange attractor

Returning to the general case $c \neq ab$, we investigate a parameter region where according to our numerical simulations a strange attractor of the type of fig. 2 exists, a necessary condition of which is that the crisis point (an extension of that found in the one-dimensional limit) is not yet arrived. Owing to the symmetry of (2.10) it is sufficient to study a half-plane only: we shall consider points with positive x coordinates. In this region the equations

$$(ab - c)x^\beta = b(x' + 1) - c(y' - d), \qquad (4.1)$$

$$(ab - c)yx^\delta = -(x' + 1) + a(y' - d) \qquad (4.2)$$

are equivalent with (2.10).

First, we investigate the asymptotic shape of the strange attractor at the backbone of the Cantor book (at D^+). Therefore, we take the limit $x \to 0$ ($x' \to -1$, $y' \to d$) with the assumption that the point (x, y) belongs to the strange attractor. Here we use the fact supported by numerical simulations (see fig. 2) that the strange attractor consists of several branches crossing the y-axis at different

points. In particular, we consider a branch with the intersection coordinate y_0 (y_0 assumes positive and negative values as well). This will be mapped into another branch joining D^+. In other words, the branches at the backbone can be indexed by the y_0 value of their immediate preimage. In what follows we shall speak always about such branches.

Considering now the limit $x \to 0$ for points along a certain branch, one may set for the leading terms asymptotically $y = y_0$ in (4.2) resulting in

$$\left(\frac{b(x' + 1) - c(y' - d)}{ab - c} \right)^\delta$$

$$= \left(\frac{a(y' - d) - (x' + 1)}{y_0(ab - c)} \right)^\beta. \qquad (4.3)$$

Eq. (4.3) yields the relation required between the coordinates on a branch of the strange attractor near the backbone of the Cantor book. The shape of these curves depend sensitively on the ratio δ/β. Therefore, the following cases can be distinguished:

i) $\beta < \delta$. Taking the limit $x' \to -1$, $y' \to d$, the right hand side dominates in (4.3), i.e. the curve $x'(y')$ touches the straight line $x' + 1 = a(y' - d)$. The asymptotic form is given by

$$x' + 1 = a(y' - d) - y_0(ab - c)(y' - d)^{\delta/\beta} \quad (4.4)$$

as it follows from (4.3) recursively. Eq. (4.4) has the consequence that the maximal value y_{max} of the intersection coordinates y_0 defines the lowest lying branch (remember $ab > c$), while $-y_{max}$ the highest one. In other words, the outhermost lines of the strange attractor are given at D^+ by $x = -1 + a(y' - d) \pm y_{max}(ab - c)(y' - d)^{\delta/\beta}$, $y' > d$. As a special case this implies that the strange attractor of the Lorenz model possesses a sharply peaked shape, without any loops, at the backbone of the Cantor book (as on fig. 2a).

ii) $\beta = \delta$. Now

$$x' + 1 = \frac{a + cy_0}{1 + by_0}(y' - d). \qquad (4.5)$$

iii) $\beta > \delta$. The left-hand side dominates (4.3), i.e. the branch is tangent to the straight line $x' + 1 = (c/b)(y' - d)$. The leading contribution now reads: $(b \neq 0)$

$$x' + 1 = \frac{c}{b}(y' - d) + \left(a - \frac{c}{b}\right)\left(\frac{y' - d}{y_0 b}\right)^{\beta/\delta}. \quad (4.6)$$

Branches characterized by a negative y_0 are now defined in the region $y' < d$. Consequently, the deepest point of the strange attractor is never D^+ itself. This is an extension of the property that $\Delta > 0$ in the one-dimensional limit. The lower and upper boundary lines of the strange attractor near D^+ are now given by the curves with y_{max} and y_{min}, respectively, where y_{min} stands for the smallest positive y_0 value. Two sharply peaked shapes, from opposite directions, are now joined at D^+. One may speak in such situations about "open" Cantor books (see fig. 2b). Finally, we note that for $b = 0$ the asymptotic behaviour is given by

$$x' + 1 = y_0 c(y' - d)^{\delta/\beta} + a(y' - d) \quad (4.7)$$

as one sees directly from (4.3).

It is to be stressed that the formulas above are valid for any parameter values in a sufficiently small neighbourhood of the backbone of the Cantor book.

The picture obtained so far may be completed by observing that a global description is also possible, at least approximately, if the strength of the Jacobian (2.11) is small. As the shape is exactly known in the limit of an identically vanishing Jacobian, a perturbative method similar to that of Bridges and Rowlands [27] can be used. We consider $\varepsilon = ab - c$ as a small parameter. Then, in a first order calculation it is sufficient to replace x and y in (4.1) or (4.2) by the formulas obtained in the one-dimensional limit. Recalling that $y = (x \pm (1 + ad))/a$ and eliminating x through (3.1), (3.2) we find for the branches connected with D^+

$$x' + 1 = a(y' - d) - \frac{\varepsilon}{a}\left(f_\pm^{-1}(y' - d) \pm (1 + ad)\right)$$
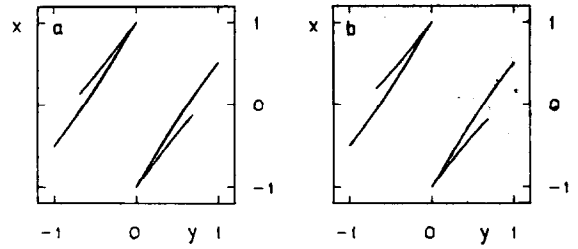$$\times \left(f_\pm^{-1}(y' - d)\right)^\delta, \quad (4.8)$$

Fig. 4. a) The strange attractor of the map (2.10) at $\beta = 0.8$, $\delta = 0.9$, $a = 1.5$, $b = 0.2$, $c = d = 0$ as obtained in a numerical simulation. b) The approximate global shape given by (4.8) at the same parameter values.

where $f_\pm^{-1}$ denotes the inverse of $f_\pm$ (see fig. 3). The domain of the different branches follows from the restrictions (3.3), (3.4). Thus, the endpoint of the $-$ ($+$) branch of (4.8) turns out to be the y coordinate of the first (second) image of the maximum point $(1 + a\Delta, -d + \Delta)$. Fig. 4b shows the approximate shape obtained by this method for a case with $\beta < \delta$. In spite of the fact that ε is relatively large and (4.8) gives the first correction only, the global agreement with the numerical result is remarkable good.

The exact calculation of the coordinates y_0 appearing in the asymptotic formulas (4.3)–(4.7) seems to be hopeless since the intersection points form a Cantor like set. The approximate global description, however, sketched above makes an approximate calculation of certain typical points (e.g. those of y_{max} or y_{min}) possible.

5. Probability density around the backbone of the Cantor book

Let us assume that the map possesses the property of hyperbolicity. Then, the attractor consists of unstable manifolds (see Sinai [28]). The invariant distribution is obtained by averaging over any of these unstable manifolds provided the density of the measure on them is suitable constructed [28]. We do not need this construction explicitly only its property as follows. Let us denote by $\tilde\rho(x, y)$ the density of such a suitable constructed measure on the unstable manifold belonging to the

point P. Then, the image of $\bar{\rho}$,

$$\rho(x', y') = \frac{\bar{\rho}(x, y)}{\lambda(x, y)}, \qquad (5.1)$$

where (x', y') is the image of (x, y), is the density of such a measure on the unstable manifold belonging to the image point of P. Here

$$\lambda(x, y) = \left[\frac{(dx')^2 + (dy')^2}{(dx)^2 + (dy)^2} \right]^{1/2} \qquad (5.2)$$

represents the coefficient of expansion [28]. In a more explicit form

$$\lambda(x, y) = \left(\frac{(d_{11}q + d_{12})^2 + (d_{21}q + d_{22})^2}{1 + q^2} \right)^{1/2}, \qquad (5.3)$$

where d_{ij} and q, both function of x and y, denote the elements of the derivative matrix of the map and the slope dx/dy, respectively.

Hyperbolicity at $D^{\pm}$ requires $\min(\beta, \delta) < 1$ as it follows from (2.10) and (5.3). Less is known about the hyperbolicity property of the whole map. The hyperbolicity property for the Poincaré section of the Lorenz model at a certain value of the parameters has been numerically proven in [9] and one may expect it to be valid in (2.10) for $\beta < \delta$, $\beta < 1$. Having in mind the possibility that the scheme above may be valid under less stringent conditions than that of hyperbolicity everywhere on the attractor, we apply it also for the other cases in order to make possible a comparison with the results obtained in the limit of strong dissipation.

We proceed by assuming that $\bar{\rho}(x, y)$ remains finite in the limit $x \to 0$ along any fibres, which is supported by the numerical observations. The particular branch of the unstable manifold we investigate crosses the y-axis at a certain coordinate y_0 under the slope q_0. In the limit $x \to 0$ d_{11} and d_{21} dominate (5.3) as it follows from (2.10), and y can be replaced by y_0.

The particular behaviour depends again strongly on the ratio of β and δ, therefore, the following cases are to be distinguished:

i) $\beta < \delta$. Expressing x in terms of x' and y' by (4.1) and using (4.4) for the asymptotic shape we find for the density as a function of the coordinate x' along the fibre

$$\rho(x') \sim \left(\frac{1 + x'}{a} \right)^{(1-\beta)/\beta}$$

$$\times \left[1 - \left(\frac{1 - \beta}{\beta} \frac{c}{a} + \frac{b + ac}{1 + a^2} \frac{\delta}{\beta} \right) y_0 \left(\frac{1 + x'}{a} \right)^{(\delta - \beta)/\beta} \right]. \qquad (5.4)$$

ii) $\beta = \delta$. From (4.1) and (4.5) one obtains

$$\rho(x') \sim (1 + x')^{(1-\beta)/\beta}. \qquad (5.5)$$

iii) $\beta > \delta$. Using now (4.2) and (4.6) we find for $c \neq 0$

$$\rho(x') \sim \left(\frac{1 + x'}{y_0 c} \right)^{(1-\delta)/\delta}$$

$$\times \left[1 - \left(\frac{1 - \delta}{\delta} \frac{a}{c} + \frac{b + ac}{b^2 + c^2} \frac{\beta}{\delta} \right) \frac{1}{y_0} \left(\frac{1 + x'}{y_0 c} \right)^{(\beta - \delta)/\delta} \right]. \qquad (5.6)$$

If $c = 0$ it follows from (4.2) and (4.6) that

$$\rho(x') \sim \left(\frac{1 + x'}{a} \right)^{(1-\delta)/\beta}$$

$$\times \left[1 - \frac{1 - \delta + \beta}{\delta} \frac{1}{y_0 b} \left(\frac{1 + x'}{a} \right)^{(\beta - \delta)/\beta} \right]. \qquad (5.7)$$

(If b also vanishes (5.5) is valid.)

For $|\delta - \beta| > 1$ the linear corrections to the prefactors (e.g. $q = q_0 + q_1 x$ in (5.3)) dominates the terms in the square brackets of (5.4)–(5.7), therefore, the next to leading terms are then characterized by other power laws which can also be easily calculated. By setting $c = ab$ and taking into consideration that the intersection point with the positive x axis is then $y_0 = (1 + ad)/a$, the for-

mulas (5.4) and (5.6) are equivalent with (3.15) and (3.17), respectively.

Acknowledgements

Appendix A

We consider the dynamics

$$
\begin{aligned}
x' &= -1 + \frac{(1 + l_1)^2}{2l_1} x \pm \frac{1 - l_1^2}{2l_1} x, \quad x > 0, \\
x' &= 1 + \frac{(1 + l_2)^2}{2l_2} x \pm \frac{1 - l_2^2}{2l_2} (-x), \quad x < 0,
\end{aligned}
\tag{A.1}
$$

where the sign in front of the last terms are identical with that of the preimage of x, and l_1 and l_2 are positive constants less than 1. At any choice of l_1 and l_2 a fully developed chaos case is realized.

As now

$$
\begin{aligned}
\phi_1 &= -1 + x(1 + l_1)/l_1, \quad \phi_2 = -1 + x(1 + l_1), \\
\phi_3 &= 1 + x(1 + l_2), \quad \phi_4 = 1 + x(1 + l_2)/l_2,
\end{aligned}
\tag{A.2}
$$

one finds by observing (3.8) that a piecewise constant solution exists:

$$
P_+(x) = \begin{cases} p, & -1 < x < l_1, \\ 0, & l_1 < x < 1, \end{cases}
$$

$$
P_-(x) = \begin{cases} p, & -l_2 < x < 1, \\ 0, & -1 < x < -l_2. \end{cases}
\tag{A.3}
$$

Thus

$$
\begin{aligned}
P(x) &= P_+(x) + P_-(x) \\
&= \begin{cases} p, & -1 < x < -l_2 \quad \text{and} \quad l_1 < x < 1, \\ 2p, & -l_2 < x < l_1, \end{cases}
\end{aligned}
\tag{A.4}
$$

with $1/p = 2 + l_1 + l_2$.

The expression of the Lyapunov number is given by

$$
\begin{aligned}
\bar{\lambda} = &\int_0^{l_1} P_+(x) \ln|\phi_1'(x)| dx \\
&+ \int_0^1 P_-(x) \ln|\phi_2'(x)| dx \\
&+ \int_{-1}^0 P_+(x) \ln|\phi_3'(x)| dx \\
&+ \int_{-l_2}^0 P_-(x) \ln|\phi_4'(x)| dx.
\end{aligned}
\tag{A.5}
$$

After substitution one obtains

$$
\begin{aligned}
\bar{\lambda} = \frac{1}{2 + l_1 + l_2} &\left(l_1 \ln \frac{1 + l_1}{l_1} + l_2 \ln \frac{1 + l_2}{l_2} \right. \\
&\left. + \ln\left[(1 + l_1)(1 + l_2)\right] \right).
\end{aligned}
\tag{A.6}
$$

For $l_1 = l_2 = 1$ the Bernoulli shift is recovered.

Appendix B

In this appendix we discuss shortly the phenomenological question how can the map (2.10) be generalized so that its most important properties remain unchanged. First, we note that by introducing

$$
z = (cy - bx)/(b + cd)
\tag{A.7}
$$

(2.10) may be rewritten as

$$
\begin{aligned}
x' &= \left(-1 + a|x|^\beta + b|x|^{\delta+1}\right) \\
&\quad \times \operatorname{sgn}(x) + z(b + cd)|x|^\delta, \\
z' &= \left(1 - |x|^\beta (ab - c)/(b + cd)\right) \operatorname{sgn}(x).
\end{aligned}
\tag{A.8}
$$

A straightforward extension of (A.8) is then

$$x' = f(|x|)\,\text{sgn}(x) + zg(|x|),$$
$$z' = h(|x|)\,\text{sgn}(x),$$
$$(A.9)$$

where f, g and h are independent functions. In order to find Cantor book structure we require that g vanishes at the origin. The branches of the strange attractor are then pinched together at $(f(0), h(0))$. The Jacobian is now $J(x) = -g(|x|)\,\mathrm{d}h(|x|)/\mathrm{d}|x|$.

We concentrate again on a neighbourhood at the backbone of the Cantor book supposed to be situated at $(\mp 1, \pm d)$. The local forms of the functions f, g, h are chosen for $x \to 0^+$ as

$$f(x) = -1 + ax^k, \quad g(x) = cx^\delta,$$
$$h(x) = x^\beta + d,$$
$$(A.10)$$

where k, δ, $\beta > 0$. The main difference between the present case and map (2.10) is that k now need not coincide with β. Since z' is a function of x only, the asymptotic shape of a branch of the strange attractor at $(-1, d)$ reads

$$x' + 1 = a(z' - d)^{k/\beta} + cz_0(z' - d)^{\delta/\beta}, \quad (A.11)$$

where z_0 denotes the intersection coordinate of the preimage branch with the z-axis. Whether the Cantor book is open depends on the ratios of the exponents.

From (5.3) and the elements of the derivative matrix of (A.9) follows that d_{11} and d_{21} dominate again (5.3). One obtains for $z' \to d$

$$\rho(z') \sim \Big[\big(ak(z' - d)^{(k-1)/\beta}$$
$$+ c\,\delta z_0(z' - d)^{(\delta-1)/\beta} \big)^2$$
$$+ \beta^2(z' - d)^{2-2/\beta} \Big]^{-1/2}. \quad (A.12)$$

A new type of behaviour arises for $k < \beta, \delta$ with a leading exponent $(1 - k)/\beta$.

References

[1] M. Hénon, Commun. Math. Phys. 50 (1976) 69.
[2] P. Holmes, Phil. Trans. of the Royal Society 292 (1979) 419.
[3] E.N. Lorenz, J. Atmospheric Sci. 20 (1963) 130, 167.
[4] J. Guckenheimer, in: The Hopf Bifurcation and Its Applications, J.E. Marsden and M. McCracken, eds (Springer, New York, 1976).
[5] R.F. Williams, Lecture Notes in Math. 615 (1977) 94.
[6] O.E. Lanford, Limit Theorems in Statistical Mechanics, Troisième Cycle de la Physique, E.N. Suisse Romande, Semestre d'Eté 1978.
[7] J. Guckenheimer and F. Williams, Publ. Math. IHES 50 (1979) 307.
[8] J. Guckenheimer, J. Moser and S.E. Newhouse, Dynamical systems (Birkhäuser, Boston, 1980).
[9] Ya. G. Sinai and E.S. Vul, Physica 2D (1981) 3.
[10] M. Hénon and Y. Pomeau, Lecture Notes in Math. 565 (1976) 29.
[11] M.I. Rabinovich, Sov. Phys. Usp. 21 (1978) 443.
[12] O.E. Rössler, Z. Naturforsch. 31a (1976) 1664.
[13] D. Ruelle, Lecture Notes in Math. 565 (1976) 146.
[14] J.A. Yorke and E.D. Yorke, J. Stat. Phys. 21 (1979) 263.
[15] J.L. Kaplan and J.A. Yorke, Comm. Math. Phys. 67 (1979) 93.
[16] A. Arneodo, P. Coullet and C. Tresser, Phys. Lett. 81A (1981) 197.
[17] Y. Kuramoto and S. Koga, Phys. Lett. 92A (1982) 1.
[18] D.V. Lyubimov and M.A. Zaks, Physica 9D (1983) 52.
[19] L.P. Shilnikov, Math. USSR Sbornik 6 (1968) 427.
[20] G. Györgyi and P. Szépfalusy, J. Stat. Phys. 34 (1984) 451.
[21] M.J. McGuinness, Phys. Lett. 99A (1983) 5.
[22] R. Graham and H.J. Scholz, Phys. Rev. A 22 (1980) 1198.
[23] M. Dörfle and R. Graham, Phys. Rev. A 27 (1983) 1096.
[24] C. Grebogi, E. Ott and J.A. Yorke, Physica 7D (1983) 181.
[25] P. Collet and J-P. Eckmann, Iterated Maps on the Interval as Dynamical Systems (Birkhäuser, Boston, 1980).
[26] M. Misiurewicz, Maps of an interval, in: Chaotic Behaviour of Deterministic Systems, G. Ioos, R.H.G. Helleman and R. Stora, eds. (North-Holland, Amsterdam, 1983).
[27] R. Bridges and G. Rowlands, Phys. Lett. 63A (1977) 189.
[28] Ya.G. Sinai, Sel. Math. Sov. Vol. 1 (1981) 100.